SHORT COMMUNICATION

3D Printed and Electrospun, Transparent, Hierarchical Polylactic Acid Mask Nanoporous Filter

Haijun He[1], Min Gao[2], Balázs Illés[3], Kolos Molnar[1,4,*]

[1]Department of Polymer Engineering, Faculty of Mechanical Engineering, Budapest University of Technology and Economics, Műegyetem rkp. 3-9, H-1111, Budapest, Hungary

[2]Department of Mechatronics, Optics and Engineering Informatics, Faculty of Mechanical Engineering, Budapest University of Technology and Economics, Műegyetem rkp. 3-9, H-1111, Budapest, Hungary

[3]Department of Electronics Technology, Faculty of Electrical Engineering and Informatics, Budapest University of Technology and Economics, Műegyetem rkp. 3-9, H-1111, Budapest, Hungary

[4]MTA–BME Research Group for Composite Science and Technology, Műegyetem rkp. 3, H-1111, Budapest, Hungary

Abstract: Face masks are becoming one of the most useful personal protective equipment with the outbreak of the coronavirus (CoV) pandemic. The entire world is experiencing shortage of disposable masks and melt-blown non-woven fabrics, which is the raw material of the mask filter. Recyclability of the discarded mask is also becoming a big challenge for the environment. Here, we introduce a facile method based on electrospinning and three-dimensional printing to make changeable and biodegradable mask filters. We printed polylactic acid (PLA) polymer struts on a PLA nanofiber web to fabricate a nanoporous filter with a hierarchical structure and transparent look. The transparent look overcomes the threatening appearance of the masks that can be a feasible way of reducing the social trauma caused by the current CoV disease-19 pandemic. In this study, we investigated the effects of nozzle temperature on the optical, mechanical, and morphological and filtration properties of the nanoporous filter.

Keywords: Coronavirus disease-19, Electrospinning, Mask nanoporous filter, Nanofibers, Three-dimensional printing

***Corresponding Author:** Kolos Molnar, Department of Polymer Engineering, Faculty of Mechanical Engineering, Budapest University of Technology and Economics, Műegyetem rkp. 3-9, H-1111, Budapest, Hungary; molnar@pt.bme.hu

***Received*:** April 19, 2020; ***Accepted*:** May 18, 2020; ***Published Online*:** July 1, 2020

(This article belongs to the *Special Section: Research and Applications of 3D Printing and Bioprinting for Covid-19*)

Citation: He H, Gao M, Illés B, *et al.*, 3D Printed and Electrospun, Transparent, Hierarchical Polylactic Acid Mask Nanoporous Filter*, Int J Bioprint*, 6(4): 278. DOI: 10.18063/ijb.v6i4.278.

1 Introduction

There are various biological aerosol particles in the outdoor air, including viruses, bacterial cells, bacterial and fungal spores, fragments, and pollen grains which may cause health issues, especially infectious diseases[1]. These particles of small sizes can easily penetrate the human respiratory system and cause flu, colds, pneumonia, and others. For example, the diameter of the 2019-novel coronavirus (nCoV) particles varies from about 60 to 140 nm[2], which poses a threat to global public health. One of the latest studies has indicated that surgical masks can prevent transmission of human CoVs from symptomatic individuals[3]. Therefore, it is essential and practical to wear personal protective equipment (e.g., face masks and respirators) during the outbreak period[4]. In general, good quality face masks are comprised of 3-4 textile layers. Melt-blown PP microfibers are widely used as the filter layer to capture the particles. However, to fulfill the requirement of

© 2020 He, *et al*. This is an Open Access article distributed under the terms of the Creative Commons Attribution-NonCommercial 4.0 International License (http://creativecommons.org/licenses/by-nc/4.0/), permitting all non-commercial use, distribution, and reproduction in any medium, provided the original work is properly cited.

mask with high filtration efficiency, the thickness of the filter has to be increased due to its microsized fiber diameter and large pore size[5]. The thickness of the mask can cause difficulty to breathe through, and as a result, the wearer will inhale unfiltered air through the edge of the mask. In comparison with melt-blown fibers, electrospun nanofiber web is an alternative candidate as a filtration media because of their small pore size, small diameter and large specific surface area. Liu *et al*.[6] prepared polyacrylonitrile (PAN)/polyacrylic acid composites nanofiber membranes as the filtration medium and it had a removal efficiency (99.994%) against the 300-500 nm NaCl aerosol particles at an airflow velocity of 5.3 cm/s. Zhang *et al*.[7] reported the use of PSU/PAN/PA-6 hybrid fibrous membranes to capture airborne particles and it can almost completely remove ~300 nm particles with an extremely small pore size of 270 nm. Most of the studies investigated the air filtration performance with 300 nm aerosol particles that are slightly bigger than the viruses. Although there is no direct measurement reported so far, we can still conclude that nanofibers are extremely good at capturing bigger airborne virions. Furthermore, severe acute respiratory syndrome-CoV-2 virus is usually transmitted by large respiratory droplets rather than by separate and individual virions. Therefore, based on the literature, the nanofiber filters can capture the vast majority of respiratory virions.

Although the electrospun nanofibers have such good advantages, including better filtration performance in the nanoscale compared with melt-blown fibers, optimizing their mechanical properties is still a big challenge. Therefore, the electrospun nanofibers must be combined with other supporting materials, for example, textile fabric, plastic mesh, and metallic mesh to make air filters[8]. Direct coating, where the electrospun nanofiber layer is deposited on the surface of the substrate, is the most common method to make such combined structure. However, there are a few issues with this process: (1) The conductive substrate can result in non-uniform deposition of nanofibers; (2) as the nanofibers are very sensitive, it is difficult to handle such flexible sheets without damaging the nanofibers; and (3) it is not possible to change such filter, so the mask can only be disposable.

Recently, three-dimensional (3D) printing technology is introduced to easily integrate nanofibers with 3D printed parts to support nanofibers. In the literature, fused deposition modeling (FDM) is the most common 3D printing technology to be combined with electrospinning[9-11]. In all these studies, the electrospun nanofibers were directly deposited onto the 3D printed objects. However, Kozior *et al*.[12] pointed out that the adhesion between the polylactic acid (PLA) printed objects and the PAN electrospun nanofibers was low. It could be better when soft TPU was used as the collecting substrate. To improve the adhesion between the nanofiber mat and the 3D printed object, the same research group[13] proposed another reverse method. They directly introduced 3D printed PLA on the electrospun PAN nanofiber mats, and it was found that the adhesion between the nanofibers and the printed polymer was stronger than the connection among the nanofibers within the nanofiber mat. However, as the nanofiber mat had glued onto the printing bed before printing, it is difficult to detach the composite, which is a big issue.

As the recyclability of disposable masks is going to become a big issue to the environment, it is necessary to make the disposable masks from biodegradable polymers urgently. It is also a good concept only if the filter within the mask is disposable, so the mask itself can be used multiple times after disinfection. PLA is the most popular material for FDM due to its easy processability and commercial availability[14,15]. It is an environmentally friendly polymer material and can be entirely biodegradable under certain conditions. Thus, the main goal of this study is to prepare PLA electrospun nanofibers combined with 3D printed PLA part for disposable filters of future masks. The layered filaments with a proper spacing support the nanofibers and simultaneously allow easy breath through. The transparent look can help to avoid the threatening appearance of the mask and can allow lipreading for people with mutism or hearing impairment.

In this study, we propose a simple transfer method to combine the nanofiber layer with a 3D printed substrate. As the printed filament and the nanofiber were made from identical material, the nozzle temperature is a crucial parameter to influence the morphology during the printing process. Therefore, we investigated the effects of nozzle temperature on the morphological, mechanical, optical, and filtration properties.

2 Materials and methods

2.1 Materials

PLA (M_w = 140,000 g/mol) (HP3100, NatureWorks LLC, USA) solution in a 10 wt% concentration was prepared by dissolving PLA pellets in a 9:1 wt. mixture of chloroform (Azure Chemicals, Hungary) and n,n-dimethylformamide (DMF, Merck). The solution was stirred at 50°C for 10 h at 250 rpm with a magnetic stirrer and then stored for 24 h. All the chemicals were used without further purification.

2.2 Sample preparation

2.2.1 Fabrication of nanofiber mat

The nanofibers were prepared with a vertical single needle electrospinning setup. The PLA solution was electrospun with the following parameters: 25 kV voltage, 0.51 mm nozzle diameter, and 20 cm distance between the needle and the grounded plate collector.

A syringe pump (Aitecs SEP-10S plus, Lithuania) supplied the PLA solution from a 20 ml syringe at a feeding rate of 0.3 ml/h. The high voltage was provided by a DC high-voltage generator (MA2000 NT 75/P, Hungary). Nanofibers were collected for 5 min (~1.0 μm thick) onto an aluminum foil.

2.2.2 Fabrication of the nanofiber filter

For the 3D printing and the electrospinning, we used the identical PLA grade to make a self-reinforced structure. Before the extrusion process, the PLA pellets were dried at 80°C for 12 h. We prepared custom filaments with a 1.75 mm diameter by extrusion. For the filament production, we used a Labtech LTE 26-44 type twin-screw extruder with a custom die. The first zone of the extruder and the die was set at 165°C and 185°C, respectively. The filaments were calibrated manually, cooled by air, and then wound up.

A CraftBot Plus (CraftUnique, Hungary) FDM printer with a nozzle diameter of 0.4 mm was used for processing the filters. The layer height and the printing speed were 0.2 mm and 50 mm/s, respectively. Even 100% infill setting results in a proper spacing between the laid filaments (struts). The porosity of the printed structure can be easily adjusted by this parameter. We set the infill density to 30% for filtration tests, as this setting made the filter even more comfortable to breathe through.

The fabrication process of the nanofiber filter is illustrated in **Figure 1**. The aluminum foil covered with the nanofiber mat was glued on the printing bed. Two layers (50 × 50 mm square) were printed directly on the nanofiber mat (30 × 30 mm) for optical transparency tests, while for the tensile tests, 30 × 10 mm samples were generated. Then, the nanofiber mat combined with the printed layers was easy to peel off from the foil without damaging the nanofiber structure. The technology allows us to make the filter in any shape (circle, oval, etc.) to fit any type of masks, and the filter is flexible.

2.3 Characterization

2.3.1 Microscopy

The morphology of the nanofibers was investigated with a scanning electron microscope (JEOL-JSM-6380 LA, Japan). The nanofiber sample was finely coated with gold-palladium (Au/Pd) alloy before the examination. We measured 100 random fibers and obtained the diameter frequency distributions using the ImageJ software. The pore size distribution was also evaluated with the same software.

We used a digital light microscope Olympus BX51M (Olympus, Hamburg, Germany) to observe the surface structure of the 3D printed nanofiber filter.

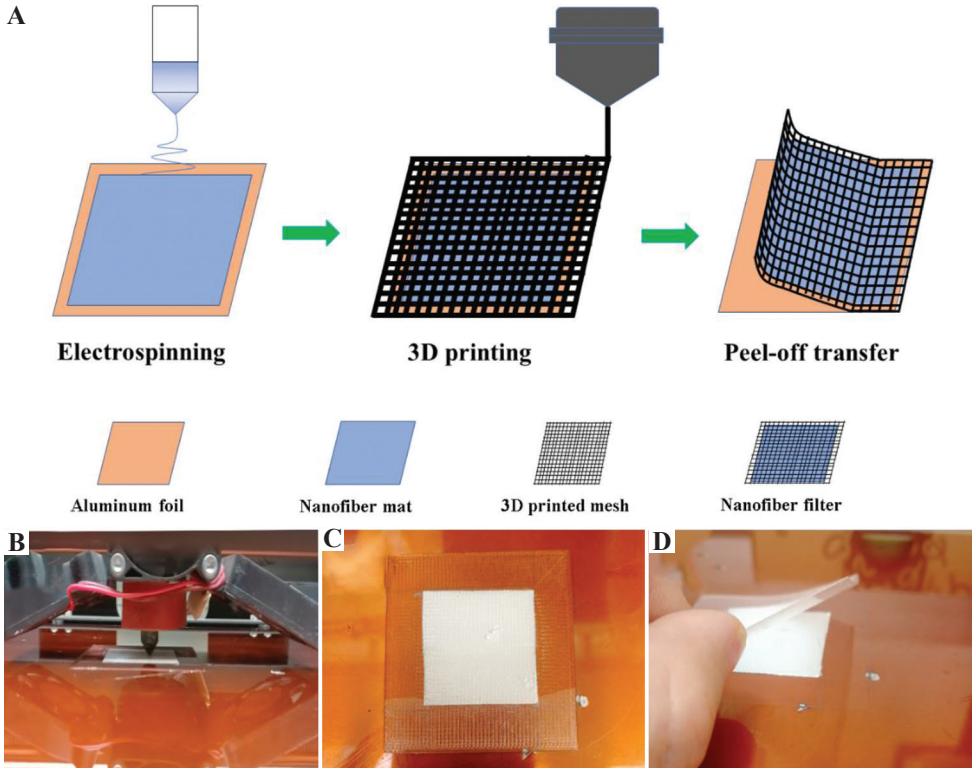

Figure 1. (A) The schematic of the fabrication of mask filter with the combination of three-dimensional (3D) printing and electrospinning, and the different components (aluminum foil, nanofiber mat, 3D printed mesh, and nanofiber filter); (B) printing in progress; (C) after printing; (D) peel-off (the sample is reflected on the base plate).

2.3.2 Optical properties

The prepared specimens were directly placed into the ultraviolet (UV) spectrophotometer (UV-1600, AOE, Shanghai, China) and analyzed at the wavelength of 200-1000 nm. Before each specimen measurement, the environment air was measured, respectively, as background.

2.3.3 Differential scanning calorimetry (DSC)

DSC was carried out with a DSC-Q2000 (TA Instruments, USA). All the samples were weighted with around 5 mg mass and sealed in an aluminum pan. They were subjected to heat/cool/heat cycles with a ramp rate of 5°C/min in the temperature range of 25°C and 200°C.

2.3.4 Mechanical properties

Tensile tests of the filters were performed with a Zwick Z005 (ZwickRoell, Germany) machine with a 5 kN load cell (0.01 N sensitivity). All the filter specimens were printed in a rectangular shape (30 mm × 10 mm × 0.4 mm). The crosshead speed and the gauge length were set at 10 mm/min and 10 mm, respectively. We measured three specimens for each group.

2.3.5 Particle filtration properties

Since the respiratory virus is airborne, we tested the filtration efficiency of the 3D printed nanofiber filters with ambient air. The particle filtering properties of the nanoporous filters were analyzed by an aerosol particle counter (Lasair III 310C, Artisan Technology Group, USA). It has six channels to detect the particle sizes of 0.3, 0.5, 1, 5, 10, and 25 μm, respectively. The PM particles in the air of our laboratory had a broad size distribution ranging from <300 nm to >25 μm. The median mass aerodynamic diameter (MMAD) of the particles in the air was between 500 and 600 nm, the size is similar to the criterion

for filtering facepieces standard tests, which works with~600 nm NaCl aerosol particles. The filtration efficiency was calculated, respectively, from particle number difference (*n*%) and mass difference (wt%) before and after 1 min filtration. Filtration efficiency (*n*%) was used to describe the filtration performance with different particle sizes. Filtration efficiency (wt%) was mainly used to evaluate the particle removal ability of a mask for particles between 0.3 and 5 μm because they are the most harmful particulate matter pollutants to humans and can reach the lower respiratory tract. The nanoporous filters were printed into a 35 mm diameter circular shape and fixed into the filter holder connected to the particle counter. All the tests were conducted with an airflow of 30 l/min, which is approximately the average breathing flow of humans in a resting position. Five specimens were tested from each sample type. As good quality commercial masks contain several filtering layers, we also stacked the specimens in 2, 3, 4, and 5 layers after the single layer measurements.

4. Results and discussion

Figure 2A presents the morphology of electrospun PLA nanofibers. The average fiber diameter was 825.2 ± 80.0 nm. **Figure 2B** shows the DSC curve of the PLA nanofiber mat. We found that the glass transition and melting temperature of the PLA nanofibers were 60.5°C and 174.3°C, respectively. We also observed a broad peak related to cold crystallization at around 85°C. To keep the stable properties of the nanofibers, but achieve proper adhesion with the printed layer, we adjusted the bed temperature to 60°C.

The optical properties of all the filters printed with variable nozzle temperatures are shown in **Figure 3**. On the black background, the whitish nanofiber mat incorporated with the printed part was visible, as shown in **Figure 3A**. Compared with the reference samples without nanofibers, our university logo underneath the filter was a little bit blurry, but visible, as shown in **Figure 3B**. The UV–visible spectra were measured to examine the transmittance of the printed nanocomposite quantitatively. The results are shown in **Figure 3E**. It is worth noting that the reference sample (without nanofibers) presented better optical transmittance, and the reference sample printed at 210°C had the lowest transmittance amongst the references. In comparison with the reference samples, the fabricated filters had lower transmittance. The reason for the lower transmittance of the printed nanocomposite may be due to the nanofiber mat was suspended between the gaps between the printed struts, as shown in **Figure 3C and D**, leading to light loss caused by light reflection and scattering on the nanofiber mat. Besides, the filters printed at 220°C and 230°C became less transparent compared with the filter printed at 210°C. It can be explained that at a higher temperature, the printed strut with a lower modulus cannot support itself to suspend through the gap between the struts. Then, the strut sagged down and contacted the nanofiber mat, which increased

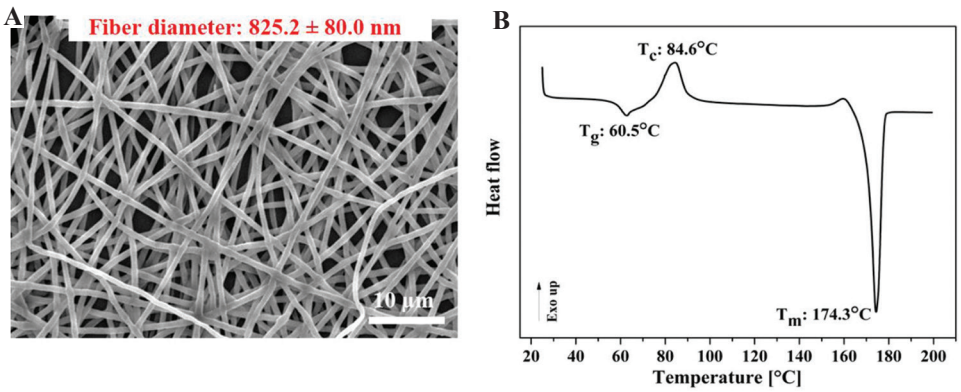

Figure 2. (A) Scanning electron microscope image of polylactic acid (PLA) electrospun nanofibers; (B) differential scanning calorimetry curve of PLA electrospun nanofibers.

the contact area between the printed strut and the nanofiber mat and reduced the porosity. Therefore, the light which went through the nanofiber mat was less. The change in the contact area is clearly seen in **Figure 3D** (230°C), in which a grid structure can be observed. This suggests that at higher temperatures, a larger interface was formed between the nanofiber mat and the printed layer. As the nanofibers were produced from the same polymer as the printing filament, we supposed that the hot printed filament might melt and destroy the nanofibers when it contacts with nanofibers. However, we observed in **Figure 3C and D** that nanofibers kept their original morphology in the printed filters, which proves that we had obtained the proper filter structure.

Figure 3F shows the typical stress-strain curves of the nanofiber filters printed with different nozzle temperatures. The results obtained from tensile testing are also listed in **Table 1**. The results presented that the tensile strength of the 3D printed nanoporous filters increases greatly as the nozzle temperature increase from 210°C to 220°C. The tensile strength slightly increased when the nozzle temperature was increased from 220°C to 230°C. Whereas the breaking strain decreased with an increase in the nozzle temperature.

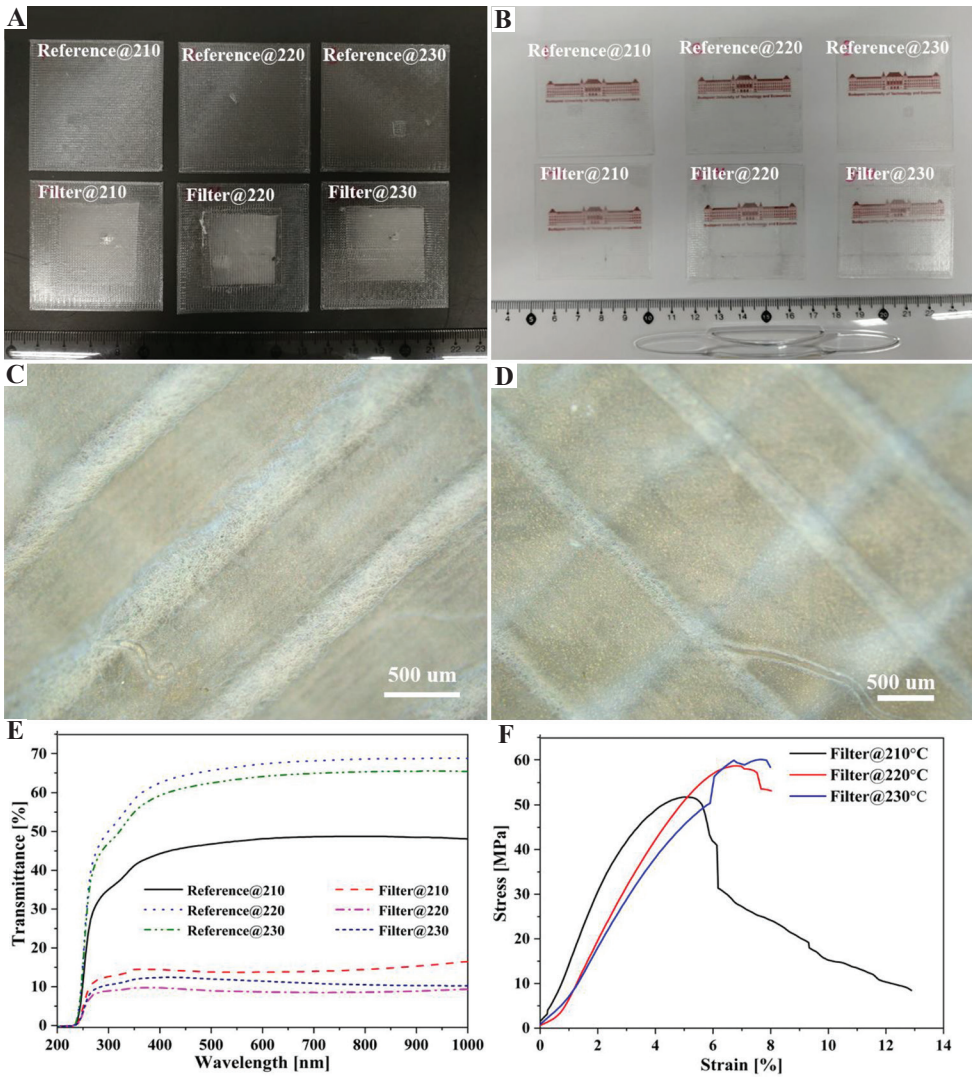

Figure 3. Optical images of the samples with different background (A) black background; (B) white background; (C) optical microscopic image of the filter with 210°C; (D) optical microscope image of the filter with 230°C (E) ultraviolet–visible spectra of the reference samples and filters; (F) the stress-strain curves of the filters with different nozzle temperatures.

Interestingly, it is noted that there was no significant change in the breaking strain when the nozzle temperature increased from 220°C to 230°C. It indicates that the nozzle temperature is a substantial factor in influencing the mechanical properties of printed nanofiber filters. It is because the higher nozzle temperature can enhance the interlayer adhesion which was also confirmed by the microscope image results. At higher temperatures, polymer chains have more mobility and take more time to form interdiffusion between the two layers. All the samples have provided proper mechanical characteristics to apply them as filters; therefore, we can conclude that the limiting factor is the change in morphology, i.e., fiber fusion.

Table 1. Main tensile properties of the 3D printed PLA filters

Nozzle temperature (°C)	Tensile strength (MPa)	Strain at break (%)
210	51.76±0.27	12.88±1.97
220	58.75±3.63	7.53±0.49
230	60.18±1.20	7.63±1.08

To evaluate the filtration efficiency of the nanoporous filters, we investigated their particle filtration properties. **Figure 4A** illustrates the filtration efficiency of the filters printed at different temperatures against the various filtered particle size (which are also summarized in **Supplementary File Table 1**). For the particle size with 5 µm and above, the filtration efficiency of the filters achieved more than 95 *n*%, except for the filter with 230°C (which had a filtration efficiency of 91.78 *n*%). For the air itself (500-600 nm MMAD), **Figure 4C** shows the single-layered specimens filtered 79 wt.%, 77 wt.%, and 66 wt.%, respectively, for 210, 220, and 230°C (the standard deviations can be found in **Supplementary File Table 2**). That means that the filters can overperform the standard surgical/sanitary masks (minimum 55% filtration efficiency at 700 nm MMAD according to the MSZ 4209 national standard).

We also found that the filters printed with higher temperatures had lower filtration efficiency when the particle size was smaller than 10 µm.

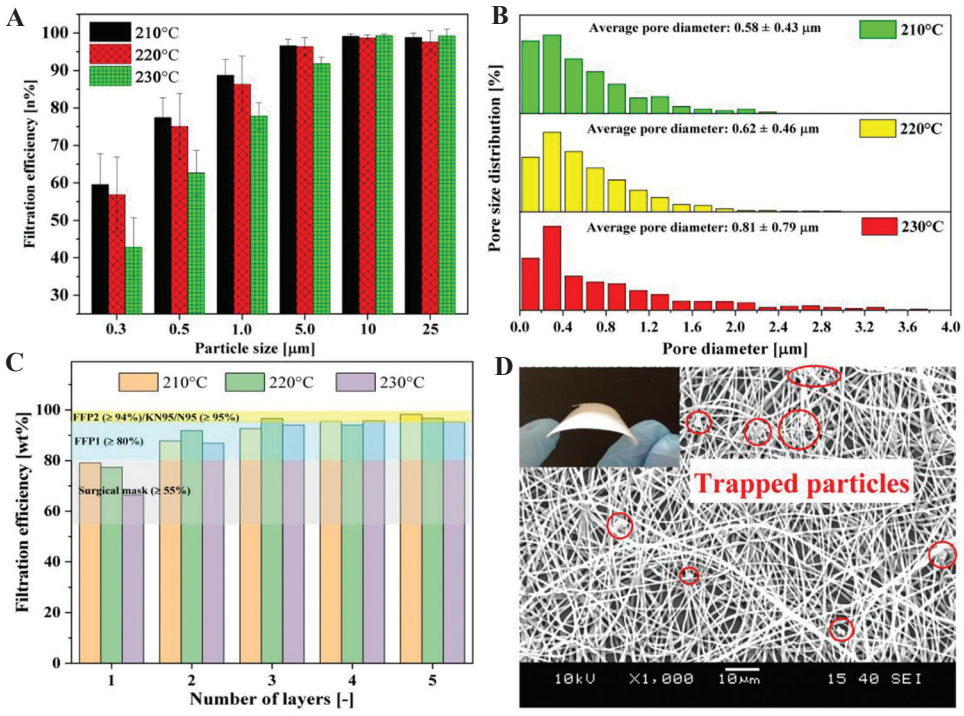

Figure 4. (A) Filtration efficiency of nanoporous filters with various particle size, (B) pore size distribution of nanoporous filter printed with different temperatures, (C) the filtration efficiency (wt%) of nanoporous filters with various stacking layers, (D) scanning electron microscope image of the nanoporous filter after filtration. Inset is the bent single-layered filter.

To understand the reason behind the observation, we evaluated the pore size distribution of all the filters (**Figure 4B**). The results of the pore size indicated that the average pore diameter of the filters with 210°C, 220°C, and 230°C was 0.58, 0.62, and 0.81 μm, respectively. The pore structure was observed at the area between the printed struts, and it was primarily determined by the electrospinning process instead of the printing temperature. Therefore, we conclude that the higher filtration efficiency was resulted from the smaller pore size and not directly related to the printing temperature. We further tested the filtration efficiency (in both [*n*%] and [wt.%]) by stacking multiple filter layers (**Supplementary file Tables 2-5**). The results we obtained are shown in **Figure 4C**. We found that a significant increase in filtration efficiency was obtained with an increase in the number of layers. Especially for the filter with 230°C, its filtration efficiency was increased from 66.32 wt.% to 95.24 wt.%. One layer performs better than a surgical mask, and two-layered filters had a filtration efficiency of more than 80 wt.%, which is the criterion for FFP1 respirators. Furthermore, when we stacked more than four layers of the filters, all of them achieved the filtration efficiency of FFP2 (≥94 wt%). Some of them even had a similar filtration performance as KN95/N95 (≥95 wt%). In **Figure 4D**, we can observe the trapped particles on the surface of the filter. The inset image shows that the printed filter was flexible and can be bent.

5 Conclusions

In this study, we introduced a simple and facile method to combine nanofiber mats to a 3D printed substrate successfully for making mask filters. Our main concept is that nanofibers give excellent filtration, while the 3D printed structure supports the fibers to avoid their damage. This technique allows printing slightly flexible mask filters in any shape achievable by 3D printing technology. The custom production also allows us to fit the mask to any face shape or to put such filters in existing masks.

As a result, we obtained a nanoporous PLA self-reinforced structure that is transparent. The transparent look overcomes the threatening appearance of the masks that can be effective in reducing the social trauma caused by the current CoV disease-19 pandemic. The transparency can also allow lipreading which can reduce communication barrier to people with mutism or hearing impairment when wearing mask. The all-PLA, self-reinforced structure renders the masks easy recyclability.

We explored the effects of nozzle temperature on the transmittance and mechanical properties of the filters developed. In comparison with the purely 3D printed mesh, the transmittance of the 3D printed filter was decreased, but they were still transparent with the transmittance around 20%. Among the filters printed with different nozzle temperatures, the filter printed at 210°C was the most transparent. The higher nozzle temperature can increase the tensile strength and decrease the breaking strain because of the better fusion between the adjacent layers. One layer can perform better than a classical surgical mask. Furthermore, the multiple layer filter can have a similar filtration performance as KN95/N95 and FFP2 filters. The results are particularly useful for future mask filter studies. Instead of stacking the layers, we can try to print the filters with multiple nanofiber layers, which can to be further investigated.

Acknowledgments

The research reported in this paper was supported by the BME-Nanotechnology FIKP grant (BME FIKP-NAT), the H2020-MSCA RISE No. 872152 - GREEN-MAP project of the European Union, the ÚNKP-17-4-I New National Excellence Program of the Ministry of Human Capacities, and the ÚNKP-19-4 New National Excellence Program of the Ministry for Innovation and Technology and BME-KKP. This paper was also supported by the János Bolyai Research Scholarship of the Hungarian Academy of Sciences and the Stipendium Hungaricum Scholarship of Tempus Public Foundation, and China Scholarship Council (201700500073).

References

1. Balazy A, Toivola M, Adhikari A, *et al*., 2006, Do N95 Respirators Provide 95% Protection Level Against Airborne Viruses, and how Adequate are Surgical Masks? *Am J Infect Control*, 34:51–7. DOI: 10.1016/j.ajic.2005.08.018.
2. Zhu N, Zhang D, Wang W, *et al.*, 2020, A Novel Coronavirus from Patients with Pneumonia in China, 2019. *N Engl J Med*, 382:727–33. DOI: 10.1056/NEJMoa2001017.
3. Leung NH, Chu DK, Shiu EY, *et al.*, 2020, Respiratory Virus Shedding in Exhaled Breath and Efficacy of Face Masks. *Nat Med*, 26:676–80. DOI:10.1038/s41591-020-0843-2.
4. Ronkay FC, 2020, The Coronavirus and Plastics. *Express Polym Lett*, 14:510–1. DOI: 10.3144/expresspolymlett.2020.41.
5. Wang SX, Yap CC, He J, *et al.*, 2016, Electrospinning: A Facile Technique for Fabricating Functional Nanofibers for Environmental Applications. *Nanotechnol Rev*, 5: 51-73. DOI: 10.1515/ntrev-2015-0065.
6. Liu Y, Park M, Ding B, *et al.*, 2015, Facile Electrospun Polyacrylonitrile/poly(Acrylic Acid) Nanofibrous Membranes for High Efficiency Particulate Air Filtration. *Fiber Polym*, 16:629–33. DOI: 10.1007/s12221-015-0629-1.
7. Zhang S, Tang N, Cao L, *et al.*, 2016, Highly Integrated Polysulfone/Polyacrylonitrile/Polyamide-6 Air Filter for Multilevel Physical Sieving Airborne Particles. *ACS Appl Mater Interfaces*, 8:29062–72. DOI: 10.1021/acsami.6b10094.
8. Xu J, Liu C, Hsu PC, *et al.*, 2016, Roll-to-Roll Transfer of Electrospun Nanofiber Film for High-Efficiency Transparent Air Filter. *Nano Lett*, 16:1270–5. DOI: 10.1021/acs.nanolett.5b04596.s001.
9. Rajzer I, Kurowska A, Jabłoński A, *et al.*, 2018, Layered Gelatin/PLLA Scaffolds Fabricated by Electrospinning and 3D Printing- for Nasal Cartilages and Subchondral Bone Reconstruction. *Mater Des*, 155:297–306. DOI: 10.1016/j.matdes.2018.06.012.
10. Naghieh S, Foroozmehr E, Badrossamay M, *et al.*, 2017, Combinational Processing of 3D Printing and Electrospinning of Hierarchical Poly(Lactic Acid)/Gelatin-forsterite Scaffolds as a Biocomposite: Mechanical and Biological Assessment. *Mater Des*, 133:128–35. DOI: 10.31224/osf.io/yt6w7.
11. Mendoza-Buenrostro C, Rodriguez CL, 2015, Hybrid Fabrication of a 3D Printed Geometry Embedded with PCL Nanofibers for Tissue Engineering Applications. *Procedia Eng*, 110:128–34. DOI: 10.1016/j.proeng.2015.07.020.
12. Kozior T, Mamun A, Trabelsi M, *et al.*, 2019, Electrospinning on 3D Printed Polymers for Mechanically Stabilized Filter Composites. *Polymers* (*Basel*), 11:2034. DOI: 10.3390/polym11122034.
13. Kozior T, Trabelsi M, Mamun A, *et al.*, 2019, Stabilization of Electrospun Nanofiber Mats Used for Filters by 3D Printing. *Polymers* (*Basel*), 11:1618. DOI: 10.3390/polym11101618.
14. Naghieh S, Badrossamay M, Foroozmehr E, *et al.*, 2017, Combination of PLA Micro-fibers and PCL-Gelatin Nano-fibers for Development of Bone Tissue Engineering Scaffolds. *Int J Swarm Intell Evol Comput*, 6:1000150. DOI: 10.4172/2090-4908.1000150.
15. Sweeney CB, Lackey BA, Pospisil MJ, *et al.*, 2017, Welding of 3D-printed Carbon Nanotube-polymer Composites by Locally Induced Microwave Heating. *Sci Adv*, 3:e1700262. DOI: 10.1126/sciadv.1700262.